Nanodomains due to Phason Defects at a Quasicrystal Surface

T. Duguet,[1,2] B. Ünal,[1,*] J. Ledieu,[2] J.-M. Dubois,[2] V. Fournée,[2] and P. A. Thiel[1]

[1]*Ames Laboratory-U.S. Department of Energy, and Departments of Chemistry and Materials Sciences & Engineering, Iowa State University, Ames, Iowa 50011, USA*

[2]*Institut Jean Lamour, UMR7198 CNRS, Nancy-Université, UPV-Metz, École des Mines de Nancy, Parc de Saurupt, CS14234, F-54042 Nancy, France*

(Received 15 December 2010; published 16 February 2011)

Among the three coexisting types of terraces found on the twofold surface of the *d*-Al-Cu-Co quasicrystal, nanodomains are essentially observed on the transition-metal rich ones, with a coherent interface boundary. Both clean surface and Ag growth analyses, demonstrate that nanodomain surfaces are structurally identical to one of the two other terraces, which contains 85 at. % Al. We provide evidence that the nanodomains are a manifestation of phason defects that extend downward toward the bulk, and state that nanodomains develop because the energetic cost of creating the phason is outweighed by the change in surface energy. Consequently, the formation of nanodomains involves more than just the surface layer, but is driven by surface energetics.

DOI: 10.1103/PhysRevLett.106.076101 PACS numbers: 68.35.Dv, 61.44.Br, 68.37.Ef

Defects in crystalline solids—deviations from an idealized structure—have always been recognized as extremely important, since they can control fundamental properties such as mechanical strength, conductivity, color and corrosion. They affect surface properties as well, such as corrosion, nucleation, or phase selection [1,2]. The relationship between surface and bulk defects has emerged recently as a topic of great importance for understanding the unusual strength of nanostructures. In nanostructures, the surfaces can cause ''dislocation starvation,'' leading to very high strength [3], but surfaces also serve as points of dislocation nucleation that ultimately allow the nanostructure to yield [4,5]. Defects in quasicrystals [6,7]—a type of ordered, but nonperiodic solids—are even more complex than in crystalline materials, since quasicrystals can contain a different type of defect, known as a phason flip [8]. In this paper, we report a new type of phason defect at the surface of a quasicrystal, a defect which bridges the bulk and the surface in an unexpected way.

A quasicrystal is a solid, often an Al-rich alloy, with good atomic order that is derived from a system other than three-dimensional periodicity. Frequently, the alternative system is described as being akin to the mathematical construction known as the Fibonacci sequence, or its geometrical analog, the Fibonacci chain [9,10]. Indeed, the analogy is not just illustrative. Manifestations of the Fibonacci chain have been observed so often in quasicrystalline materials, that they are sometimes now taken as evidence of quasicrystallinity. In surface science, for instance, evidence of surface quasiperiodicity is often taken to be the appearance of atomic-scale features arranged according to a segment of a Fibonacci chain, or values of distances (such as step heights) whose ratio equals the Golden Mean, denoted τ (vide infra).

Understanding the Fibonacci chain can help in understanding a phason, as follows. A Fibonacci chain is constructed of two objects—often chosen to be blocks that are long (L) and short (S)—, following the substitution rules: $S \rightarrow L$ and $L \rightarrow LS$. The ratio of the number of L to S objects, in the limit of an infinite chain, equals τ, an irrational number. Within this simplified picture, a phason could be a defect, such as the local inversion of an L-S pair into an S-L pair.

One previous report of phasons on quasicrystal surfaces was that of Cai *et al.* [11], who found an inversion in the sequence of high-density lines on the fivefold surface of icosahedral Al-Cu-Fe, using scanning tunneling microscopy (STM). Other studies [12,13] found regions of the twofold surface of decagonal (*d*-) Al-Ni-Co, where atomic rows were discontinuous. Nevertheless, unlike the previous observations, where phasons have been observed as highly localized defects within the surface plane, in this paper, we show a different type of phason, one which is manifest at the surface as nanodomains, but which also propagates some distance into the bulk. There is a delicate interplay between the surface and the bulk in forming this phason which is quite surprising.

To perform the experiments, a single crystal with composition $Al_{63.2}Co_{19.5}Cu_{17.3}$ was cut and polished to exhibit a surface oriented perpendicular to a [10 000] twofold axis. Details are provided elsewhere [14,15].

The surface investigated with STM using the WSxM software [16], exhibits two main types of terraces which are Al-rich and transition-metal (TM)-rich [15]. The TM-rich terraces often include nanodomains of the Al-rich structure, whereas the Al-rich terraces almost never exhibit defects of the TM-rich structure. Figs. 1(a) and 1(b) show a TM-rich terrace that includes some nanodomains, imaged

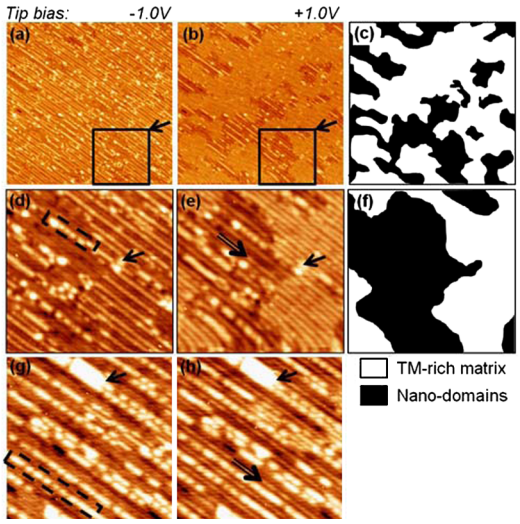

FIG. 1 (color online). STM images (100×100 nm^2) of a clean TM-rich terrace (a–b) and 33.3×33.3 nm^2 enlarged images of the insets (d)–(e) and of a clean 85 at. % Al terrace (g)–(h) Tip bias is indicated above the two first columns. Tunneling current is 0.5 nA. Panels (c) and (f) show the nanodomains (black) of images (b) and (e), respectively. Arrows serve as spatial reference points.

at opposite bias polarities. The nanodomains, and the TM-rich matrix surrounding the nanodomains, are defined in the schematic of Fig. 1(c).

Let us focus first on the TM-rich regions (the major component) of the TM-terraces. As presented elsewhere, these regions are identified as TM-rich on the basis of their atomic-scale structure, and their bias dependence in STM imaging. The presence of TM atoms at the surface, as opposed to Al atoms, leads to a stronger bias dependence [15]. This point will be key to much of the following interpretation. This interpretation is supported by experimentally-validated, calculated partial densities of states, showing that Al partial DOS is more or less symmetric around the Fermi level E_F (about $0.2 + / - 0.1$ (states/ev)/atom), whereas the TM DOS is strongly asymmetric [up to 1 (states/ev)/atom) below and about 0.1 (states/ev)/atom) above E_F][17]. Hence, over a large-scale average, the TM-rich regions in Fig. 1(a) and 1(b) show a stronger bias dependence than would be seen for an Al-rich terrace.

On a smaller scale, the effect of TM and Al atoms on bias-dependent contrast is even more striking, as revealed by the higher-magnification images of Fig. 1(d) and 1(e). Some lines in Fig. 1(d) and 1(e) are brighter at positive bias, whereas others change relatively little at the two opposite biases. One of the strongly bias-dependent lines is marked by a double-lined arrow in Fig. 1(e). The different response in the STM contrast to changing bias reflects the existence of two types of rows. And comparison with the relevant terminations extracted from Deloudi *et al.* model [18,19] shows that the *more* bias-dependent lines in Fig. 1(d) and 1(e) are pure TM rows, whereas the *less* bias-dependent lines are mixed Al-TM rows.

Focusing next on the nanodomains, the bias dependence of these features at relatively low magnification [as in Fig. 1(a) and 1(b)] is not as strong as that of the TM-rich matrix. However, examining their individual features at higher-magnification yields insight into their relationship to the TM-rich matrix. Specifically, it can be seen at positive bias [Fig. 1(e)] that some atomic lines extend straight from the TM-rich matrix into the nanodomain. One such line is marked by a double-lined arrow in Fig. 1(e).

What is the nature of the lines that penetrate straight into the nanodomains? Within the TM-rich matrix, these lines are the pure rows of TM atoms discussed above. Within the nanodomains, such lines are less bright than in the TM-rich matrix [Fig. 1(e)], but clearly retain some bias dependence. These observations suggest that within the nanodomains, the lines are a mixture of Al and TM. Structurally, this row is contiguous across the nanodomain boundaries, but chemically, there is a sharp transition. This is supported by analysis of the bulk termination of the Al-rich terrace, given below. Hence, the following picture emerges: the rows are pure TM in the TM-rich regions, but some TM atoms are replaced by Al atoms in the nanodomain, producing a mixed Al-TM row. From the viewpoint of chemical composition, this is entirely consistent with our assignment of the nanodomain as an Al-rich termination.

On the atomic scale, there is another distinctive feature of the nanodomains. This is another type of line, which is 0.10 ± 0.01 nm above the lowest plane. These lines are the brightest features in the nanodomains, and one example is enclosed by the dashed rectangle in Fig. 1(d). These lines are not bias dependent, so they are most likely made of pure Al atoms.

A portion of an 85 at. % Al terrace is shown in Figs. 1(g) and 1(h), for comparison with the nanodomains. The most striking features are the bright rows. One example is enclosed by a dashed rectangle in Fig. 1(g). These bright rows have exactly the same height and bias dependence as the bright rows in the nanodomains. Note that these bright rows are not present on the second type of Al-rich termination. Another noteworthy feature of this Al-rich terrace is the thin bright line that emerges between the bright rows at positive bias, one of which is marked by the doubleline arrow in Fig. 1(h). This has the same position (with respect to the brightest rows) and the same bias dependence, as the mixed Al-TM rows in the nanodomains (see double-lined arrow in Fig. 1(e)]. These comparisons show that the surface structure of the nanodomains is the same as the 85 at. % Al termination. According to the bulk model, the thin bright lines in Fig. 1(h) are then mixed Al-TM rows, exactly as they were assigned in the nanodomains based on their bias dependence.

Figure 2 shows a nanodomain boundary at high magnification in STM. Superimposed on the STM image is a model of atomic arrangements for the TM-rich matrix (left), and for the 85 at. % Al nanodomain (right). In the

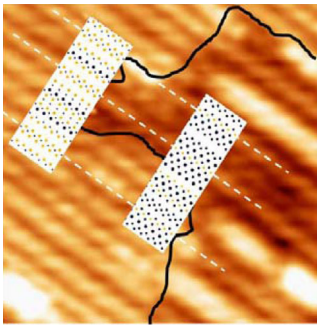

FIG. 2 (color online). TM-rich matrix-nanodomain boundary with the relevant model termination on each side. Left: TM-rich model termination. Right: 85 at. % Al model termination. Bright (orange): TM atoms, Dark (blue): Al atoms.

figure, the schematics have been selected in such a way that the pure TM rows at top left match with the mixed Al-TM rows at lower right, as seen in experiment. Of course, given that the model is quasiperiodic, other regions of the terminations could be selected where the match is not perfect. Also, the match is not unique. However, a coherent interface is achieved in the real system *and* it is possible to model it with the bulk terminations, validating our interpretation of the data.

Insight into the origin of the nanodomains can be gained by examining one that exists at a terrace step edge. This particular nanodomain also provides a good illustration of a second way to identify nanodomains: differences in Ag growth mode that depends strongly on the type of terrace that serves as the substrate [14]. Deposited Ag highlights the nanodomains, in a way that is consistent with their assignment as regions of Al-rich termination, where growth is rougher.

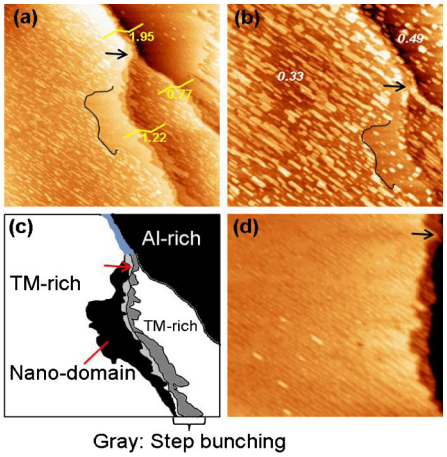

FIG. 3 (color online). STM images (500×500 nm^2) of 1.5 ML (a) and 5 ML Ag (b), grown at 365 K on twofold *d*-Al-Cu-Co (rms roughness indicated in white in (b). (d) STM image (200×200 nm^2) of some of the same region for the clean surface. (c) is a schematic of the different parts of the surface in (a–b). An incomplete contour line of a nanodomain is represented by a black line in (a)–(b). Its top boundary is marked by an arrow. Tunneling conditions are -1Vx0.5 nA.

Figure 3 shows large-scale STM images after deposition of (a) 1.5 ML and (b) 5.0 ML Ag on the two-fold surface at 365 K (imaging at the same temperature). The same area of the clean surface is shown as a reference in Fig. 3(d). The arrow serves as a spatial reference point. Above the arrow, terraces are separated by a step height of 1.95 ± 0.05 nm. The local structure on the clean terraces indicates that they are a TM-rich and an Al-rich (85 at. %) terrace, as labeled in the schematic [Fig. 3(c)].

Previous consideration of nanodomains on clean TM-rich terraces, led to the conclusion that they could be phason-related [15]. The possible surface terminations in the bulk model should be considered as surfaces of thick blocks of atoms, separated by distances following a Fibonacci sequence. A phason of the type we propose here is a localized stacking fault, i.e., a switch of two or more blocks in the perpendicular direction, within a limited lateral region. This could explain the existence of an Al-rich surface termination within a TM-rich termination, i.e., a nanodomain. Below we present, for the first time, evidence that this picture is correct.

In Fig. 3(c), the boundary between the TM-rich and Al-rich terrace starts at the top of the image as a single step. However, at the arrow—which marks the top point of the nanodomain—this step diverges, yielding a new large terrace and a step bunch where very small "terraces" can be resolved. We now analyze these step heights, both above and below the point of divergence, and over a much larger region of the surface (1000×1000 nm^2 image, not shown). Above the arrow, one finds the following sequence of step heights: $0.75 - (1.95) - 0.43 - 0.75 - 1.19 \pm 0.05$ nm. Below the arrow, the following step heights are measured: $0.75 - (1.22 - 0.77) - 0.43 - 0.75 - 1.19 \pm 0.05$ nm. (Step heights visible in Fig. 3 are in parentheses). The "1.22 nm" step height decomposes into smaller steps: $0.4 - 0.5 - 0.3 + 0.1$ nm. All of these heights can be categorized as small (S) and large (L), and combinations thereof. For this system, S and L have been determined experimentally to be 0.47 and 0.77 ± 0.05 nm, respectively [15]. Then the step sequence above the nanodomain is L-(LSL)-S-L-LS, which is a portion of a Fibonacci sequence. The step sequence at the level of the nanodomain (below the arrow) is L-(S-S-$\tau^{-1}$$S$-$L$)-$S$-$L$-$LS$, which corresponds to a faulted portion of a Fibonacci sequence, since S-S is not allowed by the substitution rules. This proves that the nanodomain in Fig. 3 is associated with a phason defect, while the TM-rich terrace, above and to the left of the nanodomain, is not.

Are the phasons related to the surface structure, the bulk structure, or both? Some arguments can be made on both sides. First, consider involvement of the bulk. The step height analysis shows that the particular nanodomain in Fig. 3 arises from a stacking fault that involves at least 2 layers of atoms beneath the surface layer; i.e., it extends at least somewhat into the bulk. Another argument for involvement of the bulk concerns the existence of a nanodomain along a step, in Fig. 3. This seems to be a fortunate

coincidence, since nanodomains are not preferentially observed at step edges. Most of them are found within terraces. This indicates that the steps are not nucleation sites, as they probably would be if the nanodomains were purely in the surface layer. From these arguments, one might think that the presence of nanodomains at surfaces is independent of the surface itself, i.e., that a phason wall exists in the bulk and the surface just happens to intersect and expose it, in the form of a nanodomain. However, a rather strong argument can be made for involvement of the surface, too. Nanodomains are almost always found on the TM-rich terraces. In our experiments, the only exceptions were a very few TM-rich nanodomains that were found on 85%-Al terraces, though it is not clear whether or not those observations were huge ''nano''-domains replacing TM-rich terraces. If the phason defects form in the bulk, then nanodomains should be present on *all* types of terminations in equal densities.

The preference for TM-rich terraces suggests that the driving force for nanodomain formation finds its source in the chemical composition of the termination. Based on chemical content alone, TM-rich terraces are expected to have higher surface energies and hence be less stable, than Al-rich ones. The development of Al-rich nanodomains is, in effect, a mechanism by which a TM-rich terrace can be replaced by an Al-rich termination. If the energetic cost of the phason is less than the cost of maintaining the TM-rich terrace, relative to an Al-rich termination, then the nanodomains will form as observed. We therefore postulate that the formation of nanodomains involves more than just the surface layer, but is driven by surface energetics.

In creating a nanodomain, an energy penalty must be paid, not only for changing the vertical stacking sequence, but also for creating the lateral boundary of the nanodomain. However, the latter term may not be too high, since (from Fig. 2) certain atomic-scale features bridge the nanodomain and the matrix.

If this picture is correct, it is not clear how or why the TM-rich terraces form at all. They must be a kind of artifact of the method of sample preparation. Such a situation is reminiscent of a previous study that revealed the existence of metastable terminations on a fivefold surface of icosahedral Al-Pd-Mn [20,21]. In that case, the metastable terminations were destroyed by removal of a two-dimensional layer across the terrace, which had the result of exposing of an underlying, and presumably more-favorable termination as the surface. The metastable terminations were observed after annealing at temperatures slightly lower than those that are normally used to obtain a well-equilibrated surface. Thus, for both fivefold *i*-Al-Pd-Mn and twofold *d*-Al-Cu-Co, it seems that metastable terminations can form during sample preparation, but they can also be removed—albeit by entirely different mechanisms.

In conclusion, we have found a type of defect at the surface of a quasicrystal, which results from the unique structure of the quasicrystal. It is a defect that is restricted to certain types of terraces, and extends toward the bulk. The data show that it reflects a defect in the stacking sequence of planes perpendicular to the surface. We postulate that nanodomains develop because the energetic cost of creating the phason and lateral interface is outweighed by the change in surface energy. Consequently, the formation of nanodomains involves more than just the surface layer, but is driven by surface energetic.

This work was partially supported by the Office of Basic Energy Sciences, Division of Materials Sciences and Engineering of the U.S. Department of Energy (USDOE) under contract DE-AC02-07CH11358, through the Ames laboratory. It was also partially supported by the European Network of Excellence on Complex Metallic Alloys (CMA) contract NMP3-CT-2005-500145 and by the Agence Nationale de la Recherche, Reference No ANR-07-Blan-0270.

*Present address: Department of Chemical Engineering, Massachusetts Institute of Technology, Cambridge, MA 02139 USA.

[1] P. Ebert *et al.*, Phys. Rev. B **67**, 024208 (2003).
[2] J. P. Pierce, N. C. Bartelt, and K. F. McCarty, Phys. Rev. Lett. **99**, 026101 (2007).
[3] J. R. Greer and W. D. Nix, Phys. Rev. B **73**, 245410 (2006).
[4] M. F. Horstemeyer, M. I. Baskes, and S. J. Plimpton, Acta Mater. **49**, 4363 (2001).
[5] W. D. Nix and S.-W. Lee, Philos. Mag., 1 (2010).
[6] J.-M. Dubois, *Useful Quasicrystals* (World Scientific, Singapore, 2005).
[7] W. Steurer, Acta Crystallogr. Sect. A **53**, 526 (1997).
[8] C. Janot, L. Loreto, and R. Farinato, Phys. Status Solidi B **222**, 121 (2000).
[9] T. Janssen, G. Chapuis, and M. de Boissieu, *Aperiodic Crystals: from Modulated Phases to Quasicrystals* (Oxford University Press, Oxford, 2007), Vol. 20.
[10] C. Janot, *Quasicrystals: A Primer* (Clarendon Press, Oxford, 1992).
[11] T. Cai *et al.*, Surf. Sci. **495**, 19 (2001).
[12] M. Kishida *et al.*, Phys. Rev. B **65**, 094208 (2002).
[13] J. Y. Park, in *Quasicrystals: Types, Systems, and Techniques* (Nova Science Publisher, Inc., 2010).
[14] T. Duguet *et al.*, Phys. Rev. B **82**, 224204 (2010).
[15] T. Duguet *et al.*, Phys. Rev. B **80**, 024201 (2009).
[16] I. Horcas *et al.*, Rev. Sci. Instrum. **78**, 013705 (2007).
[17] M. Krajci J. Hafner, and M. Mihalkovic, Phys. Rev. B **56**, 3072 (1997).
[18] S. Deloudi, Ph.D. thesis, Eidgenössische Technische Hochschule, 2008.
[19] W. Steurer and K. H. Kuo, Acta Crystallogr. Sect. B **46**, 703 (1990).
[20] B. Ünal *et al.*, Phys. Rev. B **71**, 165411 (2005).
[21] B. Ünal *et al.*, Philos. Mag. **86**, 819 (2006).